

AD718886

TRANSPORT PROCESSES IN CERAMIC OXIDES

Order No. 1130, Program Code No. 8D10

Semi-Annual Technical Report

16 June 1970 - 15 December 1970

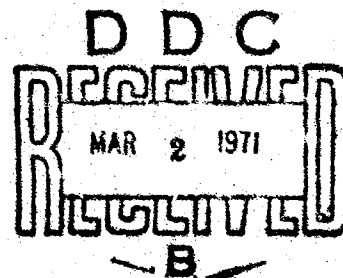
Contract No. DAHC 15-68-C-0296 (16 June 1970)

AVSD-0092-71-CR

Expiration Date: 15 June 1971

Project Scientists: T. Vasilos - 617/452-8961  
B.J. Wuensch  
P.E. Gruber  
W.H. Rhodes

Contractor: AVCO CORPORATION  
Systems Division  
Lowell, Massachusetts 01851



DISTRIBUTION STATEMENT A

Approved for public release;  
Distribution Unlimited

TRANSPORT PROCESSES IN CERAMIC OXIDES

Order No. 1130, Program Code No. 8D10

Semi-Annual Technical Report

16 June 1970 - 15 December 1970

Contract No. DAHC 15-68-C-0296 (16 June 1970)

AVSD-0092-71-CR

Expiration Date: 15 June 1971

Project Scientists: T. Vasilos - 617/452-8961  
B.J. Wuensch  
P.E. Gruber  
W.H. Rhodes

Contractor: AVCO CORPORATION  
Systems Division  
Lowell, Massachusetts 01851

### ABSTRACT

Progress is described in a program intended to clarify the nature of mass transport in MgO through (1) growth of crystals of improved perfection and purity, (2) measurement of cation self-diffusion rates over a wide range of temperatures, and (3) extension of diffusion measurements as close as possible to the melting point of the material.

Crystals of MgO 2 cm in diameter and 2 mm in thickness are routinely and reproducibly grown epitaxially on MgO substrates by means of chemical vapor transport with HCl at 1000°C. Growth rates of 90 micron/hr. have been achieved. Crystals grown from high purity source material contain 400 ppm total impurity. Primary offenders are Fe, Si and S, but it appears possible to further reduce levels of these elements. Measurements of  $\text{Ni}^{2+}$  diffusion in MgO have been extended to 2460°C ( $0.88 T_M$ ) in an attempt to reveal intrinsic transport. The measurements extend by 70% the temperature range over which transport data for MgO are now available, but fail to reveal a change in transport mechanism.  $\text{Ni}^{2+}$  diffusion at high temperatures may be adequately described by a  $D_0$  of  $1.80 \cdot 10^{-5} \text{ cm}^2/\text{sec}$  and an activation energy of 2.10 eV, a result obtained through earlier measurements at much lower temperatures.  $\text{Mg}^{26}$  self-diffusion in MgO in the temperature range 1600° - 2250°C may be represented by a  $D_0$  of  $9.52 \cdot 10^{-4} \text{ cm}^2/\text{sec}$  and an activation energy of 2.92 eV. The results are interpreted as extrinsic diffusion and are not in accord with limited data in the literature for diffusion of the radioisotope  $\text{Mg}^{28}$ . Neither of the present diffusion studies has revealed a significant difference between transport in moderate purity crystals and crystals of the best quality which are commercially available.

## TABLE OF CONTENTS

I. INTRODUCTION . . . . .	1
1.1 Mass Transport in Oxides . . . . .	1
1.2 Status of Transport in Magnesium Oxide . . . . .	2
1.3 Object and Scope of the Present Program. . . . .	4
II. CRYSTAL GROWTH AND CHARACTERIZATION . . . . .	6
2.1 Experimental . . . . .	6
2.2 Results . . . . .	7
2.3 Preparation of Diffusion Couples . . . . .	12
III. DIFFUSION IN SINGLE CRYSTAL MgO . . . . .	13
3.1 General Approach to the Problem . . . . .	13
3.2 Initial Conditions for Diffusion Specimens . . . . .	15
3.3 Exchange of Tracer with Normally-Present Isotope . . . . .	18
3.4 Materials and Specimen Preparation . . . . .	19
3.5 Diffusion Sample Analysis . . . . .	23
3.6 Results . . . . .	25
IV. REFERENCES . . . . .	31

## LIST OF TABLES

TABLE I	Mass Spectrographic Analysis of MgO (ppmw) . . . . .	8
TABLE II	Important Impurities in MgO Crystals Grown by Chemical Vapor Deposition (ppmw) . . . . .	11
TABLE III	Diffusion Coefficients for Mg <sup>26</sup> in Single Crystal MgO . . . . .	27

## LIST OF FIGURES

Figure 1.	Plot of the inverse complementary error function of $(C-C_0)/(C_s-C_0)$ as a function of Mg <sup>26</sup> penetration into single crystal MgO illustrating agreement between results obtained from different isotope ratios obtained with different mass spectrometer techniques . . . . .	29
Figure 2.	Plot of cation self-diffusion coefficients in single crystal MgO as a function of reciprocal temperature . . . . .	30

## I. INTRODUCTION

### 1.1 Mass Transport in Oxides

Many properties of materials of technological importance are controlled by mass transport. Ionic electrical conductivity, creep, sintering behavior, and oxidation or solid state reaction rates provide but a few examples of processes in which the migration rates of the constituent ions may be the rate controlling step. An understanding of mass transport rates is therefore essential in any attempt to control or interpret the kinetics of such processes.

At present, the behavior of simple ionic solids, such as the alkali and silver halides, is fairly well understood. Although such materials are still an area of active research, the availability of good crystals has permitted reliable experimental determination of the energies for defect formation and migration. The simplicity of these materials has allowed theoretical calculation of these energies, and the results are in general accord with experiment.

Extension of this understanding to more complex materials, such as oxides, has not been straightforward. Theory has been generally unsuccessful in providing estimates of the energies of defect formation and migration. Experimental work is also much more difficult. The high melting points of most oxides makes the fabrication of single crystals difficult. The energy of defect formation is higher than in monovalent solids, and crystals are accordingly less tolerant of accidentally introduced aliovalent impurities if true intrinsic transport behavior is to be observed. A few hundred parts-per-million aliovalent impurity would be sufficient to cause mass transport in most oxides to be dominated by impurities at all temperatures up to their melting points. Few, if any, oxides of the requisite purity have been available until recently. Transport measurements would

ordinarily be attempted at temperatures as close as possible to the melting point of the material in any attempt to reveal a temperature region of intrinsic behavior for a crystal of marginal purity. The high melting points of most oxides caused such temperatures to be accessible only with great difficulty. The high vapor pressure of many oxides at elevated temperatures further complicates such measurements.

A sizeable body of data exists for diffusion rates in ceramic oxides. Data are available for both anion and cation transport and, in some cases, a number of impurity cations. Such studies have provided data for commercial grade material which have proved useful in the interpretation of kinetics. Usually, however, little insight has been provided into the basic nature of the diffusion process, or even whether the transport measured represented intrinsic or impurity controlled behavior. The magnitudes of the diffusion parameters which have been observed, and purity of the materials employed, strongly suggests that impurity controlled behavior has been measured in most, if not all, studies. This has precluded study of the intentionally doped crystals which have been a key tool in understanding the defect structure of materials such as the alkali halides.

### 1.2 Status of Transport in Magnesium Oxide

The present study is concerned with a single material--magnesium oxide. This material is of considerable technological importance (e.g., as a refractory, in high temperature infrared applications, and for utilization as transparent armor). The material is of fundamental interest in that it has the simple rock salt structure and thus would appear to be an oxide to which present understanding of the alkali halides might be most readily extended. Since single crystals (although of questionable purity and perfection) have long been available, a relatively large number of

diffusion studies had been previously conducted with MgO.

Previous measurements of mass transport have been reviewed in detail in earlier reports. To briefly summarize, measurements of electrical conductivity, while having been of great value in interpreting the defect structure of alkali halides, have been of little use in clarifying the nature of mass transport in MgO. Both electronic and ionic mechanisms may contribute to conduction in oxides. MgO has been classed as a purely electronic conductor<sup>1</sup>, a purely ionic conductor<sup>2,3</sup>, and a mixed conductor<sup>4</sup> by different investigators.

Data for anion self-diffusion<sup>5</sup>, cation self-diffusion<sup>6</sup>, and for the diffusion of 8 different impurity cations<sup>7-13</sup> have been obtained for MgO. The small values of the pre-exponential term,  $D_0$ , (typically  $10^{-5}$  cm<sup>2</sup>/sec) and activation energies less than half the theoretically estimated energy for Schottky pair formation in MgO<sup>14</sup> suggest that extrinsic mass transport has been measured in all studies of impurity ion migration and in anion self-diffusion. In contrast, the data for cation self-diffusion<sup>6</sup> and Ba<sup>2+</sup> diffusion<sup>13</sup> provided larger values of  $D_0$  ( $10^{-1}$  cm<sup>2</sup>/sec) and activation energies of 3.4 eV which are reasonable parameters for intrinsic diffusion. The differences are hard to explain since (a) all studies were conducted in similar temperature ranges with materials of comparable purity, (b) the Mg<sup>2+</sup> ion has a radius comparable to that of several of the impurity ions which have been studied, and (c) the 0.9 eV energy of motion implied by the intrinsic interpretation of the data for Mg<sup>2+</sup> and Ba<sup>2+</sup> diffusion cannot be reconciled with the 1.6 to 2.7 eV activation energy observed for anion and impurity cation migration.

Interpretation of the activation energies reported is complicated by the fact that no study has revealed the change in the temperature

dependence of diffusion coefficients which would permit unequivocal identification of regions of extrinsic or intrinsic transport. The relatively high impurity concentration (ca 1000 ppm) present in the crystals employed in most studies would probably cause transport to be impurity controlled. Materials of higher purity have become available in recent years. Intrinsic transport could, in principle, be observed in such crystals at very high temperatures. To date, however, the high vapor pressure of MgO has prevented the measurement of mass transport rates at any temperature higher than two-thirds of the melting point (1850°C).

### 1.3 Object and Scope of the Present Program

The body of data obtained for mass transport in MgO to date has no unambiguous interpretation and is not self-consistent. Several studies are desirable to clarify understanding of this material. Most studies were performed at a time when available crystals contained one to two thousand ppm impurity. Recently, crystals of nominal 100 ppm impurity content have become commercially available for which it should be possible to observe intrinsic behavior at very high temperatures. It would be especially significant if a change in transport behavior could be revealed in such crystals at temperatures close to the melting point of MgO. The data for  $\text{Mg}^{2+}$  self-diffusion form the basis with which all measurements of impurity cation transport behavior must be compared. Previous data have been limited to a narrow range of temperatures for lack of a long-lived Mg radioisotope. Magnesium has three stable isotopes, however, and use of either of the three as a tracer would permit obtaining of diffusion data over a much wider range of temperatures. The main barrier to further insights into diffusion processes in oxides, however, is the lack of single crystals of the requisite purity. It would, therefore, be extremely desirable to



produce single crystals of a purity and perfection superior to those presently available.

In view of the problems described above, the present program consists of four main efforts:

- (a) Attempts to synthesize single crystal MgO of a purity and perfection superior to those presently available. Chemical transport techniques seemed especially promising and constitute the bulk of the effort in this area.
- (b) Measurement of  $\text{Mg}^{2+}$  self-diffusion rates over a wide range of temperatures, using a stable isotope as tracer to eliminate the time and temperature restrictions present in earlier experiments with a radioisotope.
- (c) Development of techniques to permit studies of impurity cation diffusion (and also cation self-diffusion) at temperatures much higher (ca 2500°C) than those previously examined in the hope of revealing a temperature range of intrinsic transport.
- (d) Thorough characterization of the purity and dislocation content of both the crystals synthesized in the program and the commercially available materials utilized in diffusion studies. Further, the manner in which such characteristics were modified in the course of specimen preparation was to be established.

Substantial progress has been made in each of these areas. MgO has been grown epitaxially on single crystal substrates with the aid of HCl transport at 1000°C. Crystals 2 cm in diameter and 2 mm in thickness have been synthesized at growth rates up to 90 micron/hr. The transport process produces deposits with lower impurity content (with two exceptions) than in the high purity source material, and the crystals being produced are

close in quality to the best specimens which are commercially available. Techniques have been developed for measuring cation self-diffusion with the aid of the stable isotope  $\text{Mg}^{26}$ . Analytical techniques using both Knudsen cell time-of-flight and triple-filament thermal ionization mass spectrometry have been perfected and reduced to practice. Cation self-diffusion data have been obtained over a temperature range of  $1600^\circ - 2250^\circ\text{C}$  and do not support interpretation given to data in the literature. Procedures have also been developed for the preparation of diffusion samples at temperatures up to at least  $2500^\circ\text{C}$ . Diffusion coefficients for  $\text{Ni}^{2+}$  in commercially available high purity  $\text{MgO}$  crystals have been obtained up to  $2460^\circ\text{C}$  ( $0.88 T_M$ ). These data extend by 70% the temperature range over which diffusion data have been conducted in  $\text{MgO}$ , but fail to provide evidence for a change in diffusion mechanism.

Technical details of the progress in each of these areas are described in subsequent sections.

## II. CRYSTAL GROWTH AND CHARACTERIZATION

In the six months covered in this report, over ninety additional samples of magnesium oxide crystals have been grown. Mass spectrometric analyses of some of the crystals grown indicate that their purity is much better than Norton crystals and nearly comparable to Spicer crystals. Reduction of the worst offenders in the grown crystals, Fe, S, and Si, would result in crystals better than the Spicer material. This reduction of these impurities appears to be possible.

### 2.1 Experimental

The experimental procedure for growing all samples during this reporting period has been the technique described previously<sup>15</sup>. The technique employs a platinum crucible with a tightly fitting cover inside

which a substrate MgO crystal is supported over a pressed pellet of the source MgO powder by means of a ring of platinum foil. In an atmosphere of anhydrous HCl at a partial pressure of 40 mm/Hg, the MgO is transported from the source to the substrate by virtue of the reversible reaction



in the thermal gradient maintained between the source MgO and the substrate crystal. The thermal gradient is achieved by heating the bottom of the platinum crucible inductively in a radio frequency coil.

The source MgO powder was Grade I Magnesium Oxide from Johnson Matthey Chemicals Limited, London. The results of the spark source mass spectrographic analysis of this material, performed by Battelle Memorial Institute, is presented in Table I.

## 2.2 Results

A number of single crystal samples 21 millimeters in diameter and as thick as 1000  $\mu\text{m}$  were grown. Some experiments were made varying the temperature gradient and source to substrate distance, in an attempt to further improve the rate of crystal growth and the properties. The results of these experiments are that smooth uniform crystals can now be made almost routinely. However, further improvement in the growth rate of 90 microns/hour, reported previously<sup>15</sup>, were not realized.

The problem encountered most frequently was a very slight brownish discoloration of the deposit. The conjecture that this discoloration might be due to platinum contamination was supported by the observation that in several cases in which the discoloration was particularly noticeable, small hexagonal platinum crystals were also observed around the periphery of the MgO deposit. Chemical transport of platinum in the HCl atmosphere

TABLE I

Mass Spectrographic Analysis of MgO  
(ppmw)

Element	Sample Designation				
	CTR 175	CTR 180	Source MgO S8573	Norton Crystal NV4	Spicer Crystal SV1
Li	0.06	< 0.002	0.6	0.2	0.06
B	(a)	(a)	0.6	(a)	(a)
F	< 5.	< 5.	< 5.	< 5.	< 5.
Na	30.	60.	60.	30.	30.
Al	20.	10.	3.	30.	20.
Si	100.	50.	5.	50.	5.
P	2.	1.	< 1.	< 1.	< 1.
S	50.	50.	200.	20.	10.
Cl	10.	10.	20.	10.	20.
K	20.	20.	10.	10.	10.
Ca	≤ 30.	≤ 30.	≤ 30.	200.	100.
Sc	< 0.1	< 0.1	< 0.1	< 0.1	< 0.3
Ti	< 5.	< 2.	< 5.	< 5.	< 5.
V	≤ 0.5	≤ 0.5	≤ 0.5	≤ 1.	≤ 2.
Cr	< 1.	< 1.	< 1.	7.	≤ 4.
Mn	5.	0.7	5.	20.	2.
Fe	150.	150.	30.	300.	50.
Co	≤ 0.4	≤ 0.4	≤ 0.4	≤ 0.4	≤ 0.4
Ni	7.	3.	7.	7.	3.
Cu	1.	0.4	1.	0.4	1.
Zn	≤ 2.	≤ 2.	≤ 2.	≤ 1.	≤ 2.
Ga	< 0.4	< 0.4	< 0.4	< 0.1	< 0.1
Ge	≤ 1.	≤ 1.	≤ 1.	< 0.4	< 0.4
As	< 0.2	< 0.2	< 0.2	< 0.2	< 0.2
Se	< 1.	< 1.	< 1.	< 1.	< 1.
Br	1.	≤ 1.	≤ 1.	≤ 1.	≤ 1.
Rb	1.	< 0.2	< 0.2	< 0.2	< 0.2
Sr	< 0.2	< 0.2	< 0.2	< 0.2	< 0.2
Y	< 0.2	< 0.2	< 0.2	< 0.2	< 0.2
Zr	6.	2.	≤ 0.5	10.	2.
Nb	< 0.2	< 0.2	< 0.2	< 0.2	< 0.2
Mo	< 1.	< 1.	< 1.	< 1.	< 1.
Ru	< 0.3	< 0.3	< 0.3	< 0.3	< 0.3
Rh	3.	< 0.1	< 0.1	< 0.1	< 0.1
Pd	< 1.	< 1.	< 1.	< 1.	< 1.
Ag	< 2.	< 2.	< 2.	< 2.	< 2.
Cd	< 1.	< 1.	< 0.3	< 0.3	< 0.3
In	< 0.3	< 0.3	< 0.3	< 0.1	< 0.1
Sn	≤ 1.	≤ 1.	≤ 1.	< 1.	< 0.3
Sb	< 0.2	< 0.2	< 0.2	< 0.2	< 0.2
Te	< 1.	< 1.	< 1.	< 1.	< 1.
I	< 1.	< 1.	< 1.	< 1.	< 1.
Cs	< 0.1	< 0.1	< 0.1	< 0.1	< 0.1
Ba	0.3	0.3	0.6	0.3	1.

TABLE I concluded

Element	Sample Designation				
	CTR 175	CTR 180	Source MgO S8573	Norton Crystal NV4	Spicer Crystal SV1
La	≤ 4.	≤ 4.	≤ 4.	< 0.1	< 0.1
Ce	≤ 2.	≤ 2.	≤ 1.	< 0.1	< 0.1
Pr	< 0.1	< 0.1	< 0.1	< 0.1	< 0.1
Nd	< 0.4	< 0.4	< 0.4	< 0.4	< 0.4
Sm	< 0.4	< 0.4	< 0.4	< 0.4	< 0.4
Eu	< 0.2	< 0.2	< 0.2	< 0.2	< 0.2
Gd	< 0.4	< 0.4	< 0.4	< 0.4	< 0.4
Tb	< 0.1	< 0.1	< 0.1	< 0.1	< 0.1
Dy	< 0.4	< 0.4	< 0.4	< 0.4	< 0.4
Ho	< 0.1	< 0.1	< 0.1	< 0.1	< 0.1
Er	< 0.3	< 0.3	< 0.3	< 0.3	< 0.3
Tm	< 0.3	< 0.3	< 0.3	< 0.3	< 0.3
Yb	≤ 5.	≤ 5.	≤ 5.	< 0.5	< 0.5
Lu	< 0.1	< 0.1	< 0.1	< 0.1	< 0.1
Hg	< 200. (b)	< 200. (b)	< 0.5	< 50. (b)	< 50. (b)
Ta	< 15. (b)	< 15. (b)	≤ 2.	< 15. (b)	< 15. (b)
W	< 50. (b)	< 20. (b)	< 0.5	< 20. (b)	< 20. (b)
Re	< 0.3	< 1.	< 0.3	< 0.3	< 0.3
Os	< 0.4	< 1.	< 0.4	< 0.4	< 0.4
Ir	< 0.2	< 1.	< 0.3	< 0.3	< 0.3
Pt	1000.	< 2.	4.	< 0.5	< 0.5
Au	< 0.5	< 0.5	< 0.5	< 0.5	< 0.5
Hg	< 0.5	< 2.	< 0.5	< 0.5	< 0.5
Tl	< 0.2	< 0.2	< 0.2	< 0.2	< 0.2
Pb	2.	2.	6.	1.	1.
Bi	0.6	0.6	0.6	0.3	0.3
Th	< 0.2	< 0.6	< 0.2	< 0.2	< 0.2
U	< 0.2	< 0.6	< 0.2	< 0.2	< 0.2

(a) Samples crushed in boron carbide mortar.

(b) Mortar contamination.

could not be the cause of the discoloration, however, since the absence or amount of discoloration varied considerably in what were thought to be duplicate experiments. Some chance observations led to the conjecture that the appearance of the discoloration was related to small air leaks into the partial vacuum inside the quartz reaction tube. This was confirmed in an experiment in which an amount of air corresponding to a pressure of 10 mm/Hg was introduced along with the 40 mm/Hg of HCl normally employed. The resulting deposit, CTR 175, was nearly black and the chemical analysis of this sample was virtually the same (Table I) as that of a colorless one (CTR 180) except for the presence of 1000 ppm of platinum. The chemical transport of platinum has been observed in oxygen<sup>16,17</sup>. Thus, the discoloration is the result of platinum impurity in the MgO deposit, brought about by the transport of platinum in a trace of oxygen which occasionally leaked into the reaction chamber.

Table I provides a complete spark source mass spectroscopic analysis of a Norton 1850°C vapor deposited crystal, a Spicer 1850°C vapor deposited crystal, the Johnson Matthey source MgO, and two Avco MgO crystals, including CTR 175, the badly discolored sample described above. Since Table I is somewhat cumbersome for a comparison of the relative concentrations of the most significant impurities, Table II lists the impurities of greatest interest.

The purity of the Avco MgO crystals is generally very much better than that of the Norton crystals. The comparison with Spicer crystals, however, shows Spicer to be slightly better. Three notable exceptions are Al, Ca, and Cl for which the Avco crystals are better than the Spicer. The low concentration of Cl in the Avco crystals is particularly significant, since contamination by the transporting agent, HCl, had been feared. Also

TABLE II

Important Impurities in MgO Crystals Grown by Chemical Vapor Deposition  
(ppm w)

<u>Element</u>	<u>CVD Crystals</u>		<u>Source MgO</u>	<u>Norton Crystal</u>	<u>Spicer Crystal</u>
	<u>CTR 175</u>	<u>CTR 180</u>			
Na	30	60	60	30	30
Al	20	10	3	30	20
Si	100	50	5	50	5
S	50	50	200	20	10
Cl	10	10	20	10	20
K	20	20	10	10	10
Ca	≤ 30	≤ 30	≤ 30	200	100
Cr	< 1	< 1	< 1	7	≤ 4
Mn	5	0.7	5	20	2
Fe	150	150	30	300	50
Ni	7	3	7	7	3
Pt	1000	≤ 2	4	≤ 0.5	≤ 0.5
Total Cation (excluding Pt)	≤ 390	≤ 345	≤ 176	670	≤ 234
Total anion	60	60	220	30	30
Total	≤ 450	≤ 405	≤ 396	700	≤ 264

gratifying is the fact that there is even considerably less Cl in these crystals than in source MgO.

The three impurities, Si, S, and Fe, are the greatest problem. Silicon may be preferentially transported from the source, although the possibility of contamination from the quartz reaction tube cannot be excluded at this time. Some reduction in sulfur is realized in the transport of MgO, which indicates that this problem could be solved by ridding the source material of some of its sulfur (possibly present as sulfate residue remaining from the preparation of the source MgO). The worst offender is clearly Fe, which is apparently being preferentially transported from the source MgO. Thus, iron contamination can probably be reduced by pre-heating the source MgO in anhydrous HCl.

### 2.3 Preparation of Diffusion Couples

The chemical transport technique lends itself very well to the preparation of diffusion couples.  $Mg^{26}$  enriched magnesia is used as the source in essentially the same apparatus used for the crystal growing experiments. The outstanding advantages of this method of preparation are that only a very small quantity of the expensive isotope-enriched MgO is necessary, and the transported MgO achieves extremely good contact with the diffusion crystal.

The diffusion crystals to be coated with the isotope-enriched MgO are smaller than the crystals used as substrates for crystal growth (6-7 mm square compared to ~25 mm). In addition, it is desirable to have the coating cover the entire face of the diffusion crystal. These two requirements necessitated slight changes in the cylindrical substrate support inside the platinum crucible. The dimensions of the substrate support for making diffusion couples was the subject of considerable



experimentation. Unenriched high purity MgO was used in these experiments. The substrate support finally arrived at, which gives excellent results, is 5 mm high (compared to 10 mm for crystal growth) and smaller in diameter, such that the diffusion crystal is supported only at the extremities of its four corners, permitting complete coverage of the diffusion face.

It is necessary to know the exact thickness of the isotope-enriched layer on the diffusion couple. It was thought that the thickness could be measured by grinding off a small amount of material perpendicular to the diffusion face from a corner of the diffusion couple to permit microscopic measurement of the deposit thickness. In the experiments with the substrate support, the "practice" diffusion couple was cleaved, perpendicular to the diffusion face, to permit microscopic examination of a profile of the deposit. Ironically, the contact between the crystal and the deposit was so good, in most cases, that the interface could not be seen. In those cases where the interface could be seen, the deposit was very uniform across the entire cleaved surface and the deposition rate was fairly consistent ( $\sim 25 \mu\text{m/hr.}$ ) for like experimental conditions. The thickness of the isotope enriched layer may therefore be determined by the exposure time in addition to direct measurement where possible.

### III. DIFFUSION IN SINGLE CRYSTAL MgO

#### 3.1 General Approach to the Problem

Diffusion coefficients may be evaluated from an experimentally determined distribution of solute which has been allowed to diffuse into a host specimen for a known time at a predetermined temperature. The analysis is readily effected if the conditions employed in the preparation of the sample are selected such that a simple analytical distribution of solute is predicted by the diffusion equation. Two types of solutes have been employed

in diffusion measurements.  $\text{Ni}^{2+}$  has been studied as an impurity cation. Concentration gradients have been determined with the aid of electron micro-beam probe spectroscopy. Study of diffusion rates of this ion were undertaken because extensive data were already available for low temperatures<sup>9,18-20</sup> and it was of interest to extend the data to higher temperatures. Micro-probe spectroscopy may be employed to analyze extremely small samples and this provided an experimental advantage in initial studies at elevated temperatures.

The lack of a long-lived radioisotope of Mg has restricted previous work on cation self-diffusion in MgO to a single study<sup>6</sup> conducted over a narrow range of moderate temperatures ( $1400^\circ - 1600^\circ\text{C}$ ). The limitation on the upper end of the temperature range was imposed by the high vapor pressure of MgO and that at the lower end by the time in which isotope penetration of an extent suitable for sectioning could be achieved without excessive decay of the tracer. ( $\text{Mg}^{28}$ , the longest-lived radioisotope, has a half-life of only 21.3 hrs.) Magnesium, however, has three stable isotopes:  $\text{Mg}^{24}$ ,  $\text{Mg}^{25}$ , and  $\text{Mg}^{26}$ , with natural abundances of 78.70%, 10.13%, and 11.17%, respectively. The use of a stable isotope as tracer offered the opportunity of eliminating the time-temperature restrictions associated with a radioisotope.

The stable isotope selected for study as solute was  $\text{Mg}^{26}$  in order that the maximum resolution in mass number relative to the most abundant isotope be obtained. The isotope, obtained from the Oak Ridge National Laboratory as a fine grained MgO powder enriched to 98.78%  $\text{Mg}^{26}\text{O}$ , was applied to a host crystal in one of three fashions described below. After an annealing the distribution of isotope was determined by the removal of thin (2 to 5 micron) layers by mechanical grinding. The isotopic

composition of each layer was determined through mass spectrometry.

The procedure has several advantages relative to conventional studies employing a radioisotope. The approach is potentially more accurate since an isotope ratio is measured, and the data are not influenced by the accidental loss of a small portion of a section. The accessibility of a wider range of temperatures for the particular system under study has already been noted. On the other hand, mass spectrometric analyses are time consuming relative to conventional counting of the activity of a radioactive section. Further, the natural abundance of the stable isotope in the host crystal provides a high "background" concentration below which solute concentrations may not be measured. This imposes rather unusual boundary conditions on the preparation of suitable specimens.

### 3.2 Initial Conditions for Diffusion Specimens

Studies of  $\text{Ni}^{2+}$  and  $\text{Mg}^{2+}$  diffusion in  $\text{MgO}$  have been conducted over a wide range of temperatures. The difference in solute characteristics and natural abundance of solute in the host crystal have necessitated use of a variety of diffusion specimens.

In a first type of specimen, an exposed surface of a  $\text{MgO}$  crystal was placed over a well cut in a crystal of the same material. The well was partially filled with either  $\text{NiO}$  or  $\text{Mg}^{26}\text{O}$ , the latter being the stable isotope used as a tracer in cation self-diffusion studies. The surface of the host crystal was thus in equilibrium with a vapor of the solute and was maintained at constant concentration throughout the course of the diffusion annealing. The distribution of solute,  $C$ , after an annealing of duration  $t$  is given by

$$C = C_s \operatorname{erfc} x (4Dt)^{-\frac{1}{2}}$$

where  $C_s$  is surface concentration,  $x$  is penetration into the specimen,  $D$  is the diffusion coefficient and  $\text{erfc}$  represents the complementary Gaussian error function. A plot of the inverse complementary error function of  $C/C_s$  as a function of solute penetration is therefore linear and has slope given by  $(4Dt)^{-\frac{1}{2}}$ . This type of specimen is subsequently referred to as a "vapor exchange" specimen. Use of the vapor exchange boundary conditions was possible only over temperature ranges in which the vapor pressure of the solute was high. In such circumstances this type of specimen provided several important advantages. The total amount of solute available in the specimen is large (compared with the finite source, thin film samples described below) and loss of solute, which may be severe at elevated temperatures where the vapor pressure of the solute is high, is less critical. Secondly, the surface of host crystal is never in contact with pure solute. This was an especial advantage in the study of  $\text{Ni}^{2+}$  diffusion where, at the highest temperature explored ( $2460^\circ\text{C}$ ) the sample preparation temperature was  $370^\circ\text{C}$  above the melting point of  $\text{NiO}$  ( $2090^\circ\text{C}$ ). Vapor exchange boundary conditions could be employed in the study of  $\text{Mg}^{26}$  diffusion at temperatures in excess of  $1600^\circ\text{C}$ . Below this temperature, the surface concentrations of isotope were not sufficiently above the natural abundance of  $\text{Mg}^{26}$  in the host crystal to permit establishment of a concentration gradient. These boundary conditions were also used in all  $\text{Ni}^{2+}$  diffusion specimens prepared at temperatures above the melting point of  $\text{NiO}$  ( $2100^\circ\text{C}$  to  $2460^\circ\text{C}$ ).

At temperatures at which the vapor pressure of the solute is too small to permit utilization of vapor exchange boundary conditions, losses of solute from a thin, finite initial film would be negligible. Solute may accordingly be supplied from a thin film. Annealing of this type of specimen produces a Gaussian distribution of solute given by

$$C = S(4\pi Dt)^{-\frac{1}{2}} \exp - x^2(4Dt)^{-1}$$

where S is the initial amount of solute per unit area. A plot of the logarithm of solute concentration as a function of the square of solute penetration is therefore linear and has slope given by  $-(4Dt)^{-1}$ . This type of sample is referred to as a "thin film" specimen. The study of  $Ni^{2+}$  diffusion employed this variety of boundary conditions at all temperatures less than the melting point of NiO.

Preparation of finite source specimens containing  $Mg^{26}$  as solute presents an unusual problem. The natural abundance of  $Mg^{26}$  is 11.17%, so that concentrations below this level are indistinguishable from "background" concentration. The concentration in the Gaussian distribution of the thin film specimen decreases as  $(Dt)^{-\frac{1}{2}}$  and approaches zero for large times. Subsequent establishment of a concentration gradient by mechanical sectioning requires a minimum detectable solute penetration of ca. 12 microns. The concentration of  $Mg^{26}O$  may be kept above background only by increasing S, the initial amount of solute per unit area. However, increasing S by the requisite amount invalidates the assumption, implicit in the thin film boundary conditions that the thickness of the initial film is negligible with respect to the extent of the solute penetration. Under these conditions the solute must be considered as being distributed throughout an initial layer of thickness, h, which is not negligible compared to the diffusion zone. Under such conditions the solute distribution is given by

$$C = \frac{1}{2}C_0 \left[ \operatorname{erf} (h-x)(4Dt)^{-\frac{1}{2}} + \operatorname{erf} (h+x)(4Dt)^{-\frac{1}{2}} \right]$$

where h is twice the thickness of the initial layer,  $C_0$  is the solute concentration in the initial layer, and erf is the Gaussian error function. This type of gradient is not as readily analyzed as those resulting from

simpler solutions to the diffusion equation. It may be noted, however, that the concentration at  $X = 0$  is given by  $C_s \operatorname{erf} h(4Dt)^{-\frac{1}{2}}$ . The surface concentration may thus be used to compute an estimate of  $(4Dt)^{-\frac{1}{2}}$ . A more accurate value based on the entire concentration gradient may be obtained by fitting the data to gradients calculated for values of  $(4Dt)^{-\frac{1}{2}}$  which are close to the initial estimate. This type of specimen is referred to as a "thick film" sample.

A final set of boundary conditions are encountered for  $\text{Mg}^{26}$  gradients at very low temperatures where the solute penetration is small compared to the thickness of the initial layer of solute. Under such conditions, a semi-infinite initial distribution of solute is approximated, and

$$C = \frac{1}{2}C_s \operatorname{erfc} x (4Dt)^{-\frac{1}{2}}$$

where  $C_s$  is concentration in the initial deposit, and  $x$  is now penetration relative to the solute-host crystal interface. A plot of the inverse complementary error function of  $2C/C_s$  is therefore linear as a function of  $x$ , and has slope given by  $(4Dt)^{-\frac{1}{2}}$ . This form of the solution to the diffusion equation is a valid approximation if  $(Dt/h^2)^{\frac{1}{2}}$  is less than about  $\frac{1}{4}$ . The semi-infinite source solution is more amenable to analysis than the thick film solution to the diffusion equation. In principle, it could be used for all temperatures for which use of the thick film conditions might be dictated. Sectioning and analysis of this type of specimen is extremely time consuming, however, and the conditions were utilized only at the very lowest temperatures at which specimens were prepared.

### 2.3 Exchange of Tracer with Normally-Present Isotopes

In the cation self-diffusion experiments a stable isotope,  $\text{Mg}^{26}$ , was diffused into a host crystal containing a natural abundance of  $\text{Mg}^{26}$

(11.17%). The initial isotopic composition of the host crystal is

$$C_o^{24} + C_o^{25} + C_o^{26} = 1$$

where  $C_o^{24}$ , the natural abundance of  $Mg^{24}O$  is .7870,  $C_o^{25}$  is .1013 and  $C_o^{26}$  is .1117. If a concentration  $X^{26}$  of isotope diffuses into the specimen, it substitutes for all three isotopes and

$$X^{26} + (1 - X^{26})(C_o^{24} + C_o^{25} + C_o^{26}) = 1.$$

The total concentration of  $Mg^{26}O$  is therefore

$$C^{26} = X^{26} + (1 - X^{26}) C_o^{26}.$$

It should be noted that the concentration of diffused tracer  $X^{26}$  is not  $C^{26}$  less the natural abundance  $C_o^{26}$ , but rather

$$X^{26} = (C^{26} - C_o^{26}) / (1 - C_o^{26}).$$

The constant factor  $(1 - C_o^{26})$ , however, cancels in analysis of all error function solute distributions since

$$\frac{X^{26}}{X_s^{26}} = \frac{(C^{26} - C_o^{26}) / (1 - C_o^{26})}{(C_s^{26} - C_o^{26}) / (1 - C_o^{26})} = \frac{C^{26} - C_o^{26}}{C_s^{26} - C_o^{26}}$$

Similarly, in the analysis of the Gaussian distribution of solute of the thin film specimen, the constant factor relating  $X^{26}$  and  $(C^{26} - C_o^{26})$  has no influence on the slope of  $\ln (C^{26} - C_o^{26})$  as a function of penetration. All concentration gradients presented in this study are therefore expressed as total concentration of  $Mg^{26}O$  less the natural abundance of  $Mg^{26}O$  even though this quantity does not represent the actual concentration of "tracer" diffused into the sample.

### 3.4 Materials and Specimen Preparation

Two varieties of commercially available single crystals of  $MgO$  have been employed in both the study of  $Ni^{2+}$  diffusion and  $Mg^{2+}$  self-

diffusion. Crystals obtained from W. & C. Spicer Ltd., Cheltenham, England, nominally contain 100 ppm impurity and represent the purest single crystals commercially available<sup>21</sup>. Less pure crystals obtained from the Norton Company, Worcester, Mass. have been employed in many earlier studies. These crystals were utilized in the present study for purposes of comparison, and also for use in early experiments as techniques for sample preparation were being perfected.

Characterization of representative crystals of both types has been described in earlier reports<sup>15</sup>. The Spicer crystals are notably superior in both purity and dislocation content. Typical Spicer crystals, analyzed by spark source mass spectrometry contained 270 pp mw total (cation plus anion, excluding  $\text{OH}^-$ ) impurity; Norton crystals contained 700 to 820 ppm w total impurity. Etch pit measurements showed both types of crystals to contain 600 to 1200 micron subgrains. Total dislocation densities in the range  $0.7 - 1.0 \cdot 10^5 \text{ cm}^{-2}$  and  $1.1 - 2.5 \cdot 10^5 \text{ cm}^{-2}$  were encountered for the Spicer and Norton materials, respectively. When the contribution of dislocations at subgrains was excluded, corresponding densities were  $2.8 - 6.7 \cdot 10^4$  and  $5.0 - 16 \cdot 10^4 \text{ cm}^{-2}$ .

Single crystals were cleaved into plates with dimensions of the order of  $1 \times 1 \times 0.3 \text{ cm}$ . As-cleaved surfaces were found to have surface roughness of 1 to 2 microns in the form of cleavage steps, and mechanical damage in the form of increased dislocation densities along intersection (110) slip bands. Mechanical polishing of the surface produced finishes which were flat to within  $\pm 0.25$  micron, but at the expense of introducing high dislocation densities in a layer within 40 microns of the surface. High temperature annealings ( $1850^\circ\text{C}$ ) succeeded in reducing the dislocation density by a factor of 2, but did not restore the native as-grown density.



Chemical polishing in hot phosphoric acid successfully removed the damaged layer, but at the expense of introducing surface "waviness". As described in previous reports<sup>15</sup>, the kinetics of material removal in such chemical polishing has been studied in detail as a function of time and temperature under static and agitated conditions. The rate of material removal increased rapidly at temperatures above 170°C. This increase corresponded to rapid development of surface pitting. Optimum polishes were achieved at 155°C in an agitated solution when the specimen was given intermittent washes in hot H<sub>2</sub>O. The best surfaces obtained had flatness inferior to mechanically polished surfaces, but represented a satisfactory compromise between roughness and minimization of surface damage.

Crystals employed for studies of Ni<sup>2+</sup> diffusion were used in the as-cleaved condition. Surface roughness and damage did not influence these results since all measurements were conducted at high temperatures at which solute penetrations were 5 to 8 times the depth of the mechanical damage introduced by cleavage. Similarly, cleaved and mechanically polished surfaces were utilized in crystals intended for Mg<sup>26</sup> diffusion at high temperatures. At low temperatures, where detectable isotope penetrations were small, mechanically and chemically polished surfaces were employed.

A matter of concern in subsequent annealing of the diffusion specimens was contamination of the high purity crystals by the furnace atmosphere, and also vaporization of the solute and diffusion interface of the host crystal. These problems were solved by encapsulation of the entire specimen in a pressed compact of high purity MgO powder. The compact sintered during the early portion of the diffusion annealing. This provided not only protection of the specimen from impurities derived from the furnace, but entrapped the solute as well.

Vapor exchange samples were prepared by partially filling a single crystal well with  $\text{Mg}^{26}\text{O}$  or  $\text{NiO}$ . A prepared surface on an  $\text{MgO}$  host crystal was placed over the well, and the assembly was then encapsulated. For thin film specimens employing  $\text{NiO}$  as solute, a layer of nickel chloride, a fraction of a micron in thickness, was deposited on a prepared surface of a  $\text{MgO}$  crystal from solution. The chloride was converted to  $\text{NiO}$  by heating at low temperature in air. Solute-crystal contact presented no problem because of the high vapor pressure of  $\text{NiO}$  at all temperatures examined. Preparation of the thick film samples necessary for the study of  $\text{Mg}^{26}$  diffusion presented difficulties. Application of the thick layer by straightforward techniques (e.g., spraying of an acidic solution, or deposition of a slurry) produced coatings which peeled from the host crystal when a thickness of  $3/4$  micron was exceeded. An additional source of concern was the impurity introduced with the  $\text{Mg}^{26}\text{O}$  isotope. The material supplied by the Oak Ridge National Laboratory also contained 0.2% cation impurity, which provided a source of contamination. Both problems were solved by utilizing the chemical vapor deposition techniques developed in the crystal growth portion of this program. An epitaxial layer of single crystal  $\text{Mg}^{26}\text{O}$  tens of microns in thickness could be deposited on a prepared surface of a host crystal in less than an hour at  $1000^\circ\text{C}$ . The temperature is low enough that the amount of diffusion during deposition is completely negligible. The procedure not only produced a single crystal layer of  $\text{Mg}^{26}\text{O}$  of the requisite thickness which was in intimate contact with the host crystal, but, as described above in Section II, effected purification of the isotope as well.

Semi-infinite source specimens utilizing  $\text{Mg}^{26}\text{O}$  as solute were also prepared by chemical vapor deposition of the isotope, by merely continuing the transport process for longer times. Such samples, being

utilized only at relatively low temperatures (ca 1000°C) were not encapsulated.

### 3.5 Diffusion Sample Analysis

The capsules containing MgO crystals in which NiO had been employed as a solute were cut upon completion of the diffusion annealing to expose a surface normal to the solute-coated interface. NiO concentrations as a function of distance normal to the interface were determined with electron microbeam probe spectroscopy. It proved necessary to coat the exposed surfaces of the specimens with a thin film of carbon to render the sample conductive and prevent charge buildup during analysis. Analyses were performed with a 30 kv electron beam having a nominal diameter of one micron. NiK $\alpha$  fluorescent intensities were recorded relative to the intensity obtained from a sample of pure Ni in order to eliminate possible errors arising from beam fluctuations. The intensity ratios were converted to concentration of NiO with the aid of a calibration curve obtained from a set of fine grained sintered NiO-MgO standards. Concentrations of solute at the surfaces of the samples ranged from .001 to .048 NiO, depending on temperature. The sensitivity of the analysis, as performed, permitted detection of concentrations as low as  $8 \times 10^{-5}$  NiO. Solute gradients could, therefore, usually be established over solute concentration ranges of two orders of magnitude.

Samples which contained Mg<sup>26</sup>O solute were removed from the capsules. Edges were ground from the host crystal to eliminate effects of surface diffusion. Sections were ground from the specimen by hand lapping on a Mo foil, using diamond powder in a small amount of alcohol as an abrasive. Parallelism of sequential sections was achieved by attaching the crystal to a cylinder of stainless steel which moved snugly within a second outer cylinder machined from the same material. Supports attached

to the outer cylinder rode on an optical flat during lapping. Tallysurf measurements of surface roughness after removal of a section showed that flatness and parallelism were maintained to  $\pm 0.25$  micron. The thicknesses of the sections removed were determined by precision weighing of the sample combined with careful measurement of the surface area of the sample. Sections less than 2 microns could be successfully removed through this procedure. In practice, section thicknesses which were removed ranged from 2 to 10 microns depending on the area of a particular sample, and the anticipated extent of isotope penetration.

The isotopic composition of each section removed from the diffusion specimen was accomplished by mass spectrometry. Such analyses are time consuming since the system must be baked out and evacuated after introduction of each one of the ten to twenty sections removed from each diffusion specimen. At best, only two analyses may be performed within a 24-hour period. Early analyses were performed with a Bendix time-of-flight mass spectrometer. During the present period of the program, these measurements have been augmented by analyses performed on a second instrument of the Mattauch double focussing type which employs a thermal ionization source.

The specimen grindings and Mo foil were placed in a tungsten Knudsen effusion cell maintained at  $1900^{\circ}\text{K}$  in the time-of-flight spectrometer. This produced a beam of magnesium atoms which was directed into the ion source of the spectrometer where it was ionized by electron impact and mass analyzed. The isotope ratio was determined by simultaneously monitoring the  $\text{Mg}^{24}$  and  $\text{Mg}^{26}$  peaks to eliminate beam fluctuations due to variations in temperature of the Knudsen cell.

In the thermal ionization technique, a portion of the grindings

were placed on the center filament of a triple filament assembly. Two side (ionization) filaments were maintained at higher temperature to provide high ionization efficiency; the center (sample) filament, which controls the rate of evaporation, was maintained at a lower temperature to produce steady volatilization. After ionization, the beam was accelerated, passed through an electrostatic analyzer to the magnetic analyzer where the  $Mg^{26}/Mg^{25}$  ratio was measured with an electronic detection system.

Both mass spectrometer techniques have been perfected to the point where either may now be used on a routine basis to analyze the small amount of material ( $5 \cdot 10^{-4}$  gram) contained in each section. Results obtained from the two different techniques are in good agreement. The accuracy of the analyses was evaluated by measurement of the isotopic abundance in normal MgO. Comparison of the results with the reported natural abundances indicated that the accuracy of the time-of-flight analyses is better than  $\pm 1\%$ , while that of the thermal ionization procedure is better than  $\pm \frac{1}{2}\%$ .

### 3.6 Results

Twenty diffusion coefficients have been obtained for  $Ni^{2+}$  diffusing in both Spicer and Norton Company MgO over a temperature range of  $1900^{\circ}$  to  $2460^{\circ}C$  ( $0.88 T_M$ ) in an argon atmosphere. No significant difference in transport behavior was noted between the Spicer and Norton material despite the superior purity and dislocation content of the former. These results extended by 70% the temperature range for which mass transport data are available in MgO, but failed to reveal conclusive evidence for a change in transport mechanism at elevated temperatures. Diffusion was assumed to be impurity controlled, and could satisfactorily be represented by

$$D = 1.80 \cdot 10^{-5} \exp -(2.10 \text{ eV/kT}).$$

This result had been obtained earlier<sup>9</sup> on the basis of measurements in air at lower temperatures. The data contained a slight suggestion of a possible change to a different transport mechanism at temperatures in excess of 2400°C. It would have been of great interest to confirm this trend with a few additional measurements at temperatures still closer to the melting point of MgO. This was unfortunately not possible in the system NiO-MgO. At 2460°C, the highest temperature at which a sample was successfully prepared, two-thirds of the NiO-MgO solid solution series was above the solidus of the system, and difficulties were experienced with melting at the sample surface. The above results were described in detail in a manuscript entitled "Diffusion of Ni<sup>2+</sup> in High Purity MgO at High Temperatures" which was attached as an Appendix to the preceding Interim Report<sup>15</sup>. The manuscript is scheduled for publication in the February 1, 1971 issue of the Journal of Chemical Physics.

A total of seven diffusion coefficients have been obtained for Mg<sup>26</sup> self-diffusion in MgO in the temperature range 1600° to 2250°C. These results are summarized in Table III. Samples have also been successfully prepared at 1950°C and 2400°C and sectioned in preparation for analysis. Mass spectrometer analyses have, in fact, been completed for 15 sections removed from the specimen which had been prepared at 2400°C. The penetration of isotope at this high temperature was so extensive, however, that the change in concentration in this depth of the crystal was insufficient to evaluate a diffusion coefficient. Additional sections are presently undergoing analysis.

As mentioned above, the rate at which mass spectrometer analyses may be performed determines the rate at which diffusion coefficients may be

TABLE III  
Diffusion Coefficients for  $Mg^{26}$  in Single Crystal  $MgO$

<u>Temp. (<math>^{\circ}C</math>)</u>	<u>Time (hrs.)</u>	<u>Material</u>	<u>Specimen Type</u>	<u><math>D(cm^2/sec)</math></u>
1600	16.0	N	V	$1.41 \cdot 10^{-11}$
1600	31.0	S	T	$1.96 \cdot 10^{-11}$
1750	16.3	N	V	$5.28 \cdot 10^{-11}$
1850	15.6	N	V	$1.48 \cdot 10^{-10}$
1850	15.6	S	V	$7.23 \cdot 10^{-11}$
2050	6.0	N	V	$3.76 \cdot 10^{-10}$
2250	5.0	N	V	$1.05 \cdot 10^{-9}$

---

N = Norton Company  $MgO$ ; S = Spicer, Ltd.  $MgO$

V = Vapor exchange specimens; T = thin film specimen

obtained. We have accordingly perfected techniques for use of a thermal ionization triple filament source on a second mass spectrometer in order to expedite analyses. After a few initial failures, these procedures have now been reduced to practice. Figure 1 presents data for a vapor exchange specimen prepared at 2050°C, in which the inverse complementary error function of  $(C-C_0)/(C_S-C_0)$  is plotted as a function of isotope penetration. Alternate sections were analyzed with the Knudsen cell time-of-flight spectrometer, and with the thermal ionization double-focussing instrument. The isotope ratios monitored in the two experiments were  $Mg^{26}/Mg^{24}$  and  $Mg^{26}/Mg^{25}$ , respectively. Although not the best gradient obtained in the program, the data of Figure 1 demonstrate excellent agreement between concentrations obtained by two different techniques even though different mass peaks were measured.

The diffusion coefficients obtained to date for  $Mg^{26}$  self-diffusion in single crystal MgO are plotted as a function of reciprocal temperature in Figure 2. The data may be represented by

$$D = 9.52 \cdot 10^{-4} \exp \left( -\frac{2.92 \text{ eV}}{kT} \right).$$

As in the measurements of impurity cation diffusion, there is at present no basis for ascribing significantly different transport behavior to the high purity Spicer MgO crystals. Figure 2 also includes the data<sup>6</sup> for diffusion of the radioisotope  $Mg^{28}$ . These results are given by

$$D = 2.49 \cdot 10^{-1} \exp \left( -\frac{3.43 \text{ eV}}{kT} \right)$$

and, as mentioned above, have generally been interpreted as representing intrinsic behavior. The present results do not confirm this interpretation. The activation energy of 2.92 eV is somewhat higher than that observed for impurity ion migration, but would appear to be too low to represent intrinsic



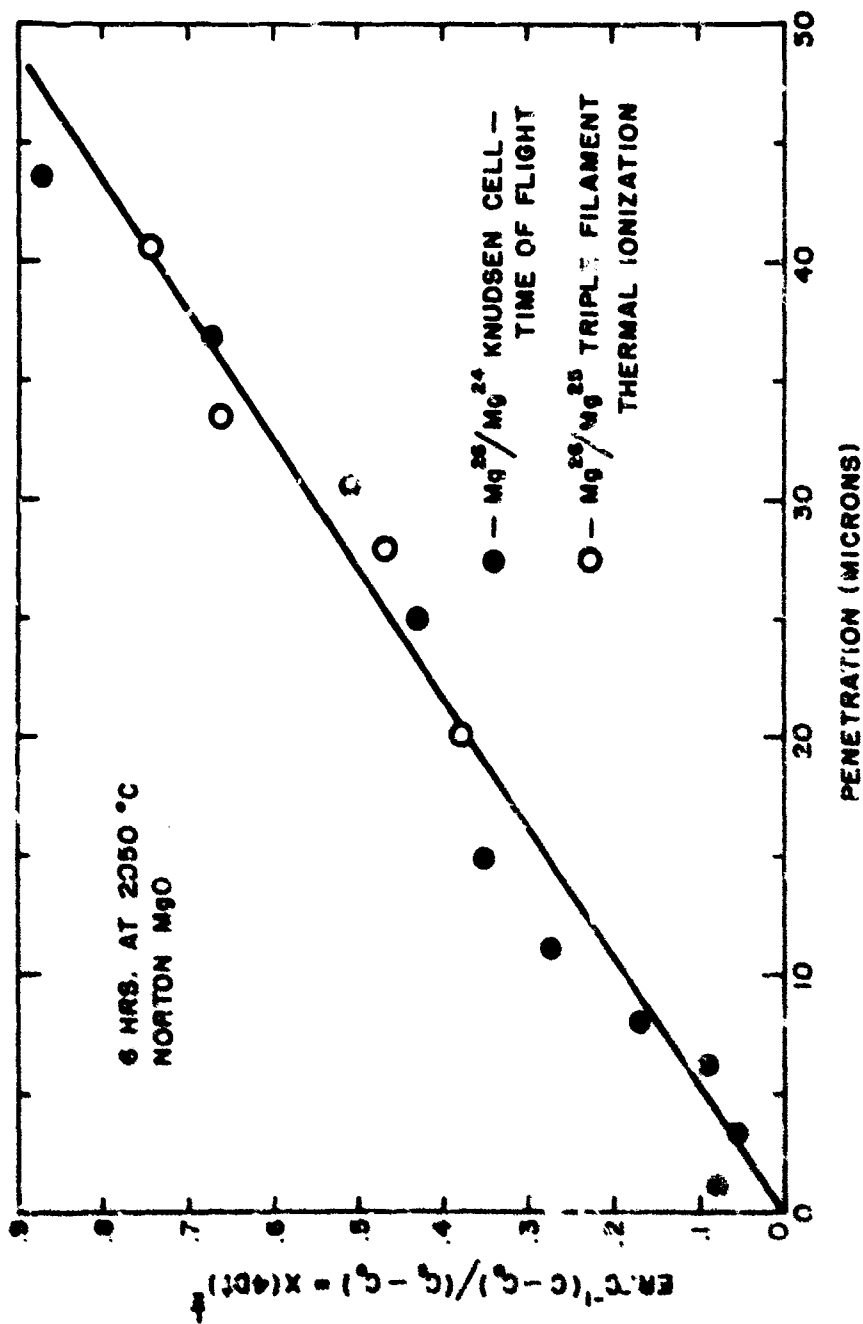


Figure 1. Plot of the inverse complementary error function of  $(C-13)/(C-12)$  as a function of  $\text{MgO}$  penetration into a crystal.  $\text{MgO}$  is a dating agent between relict and host rock. The data were obtained from different isotope ratios obtained with different mass spectrometer techniques.

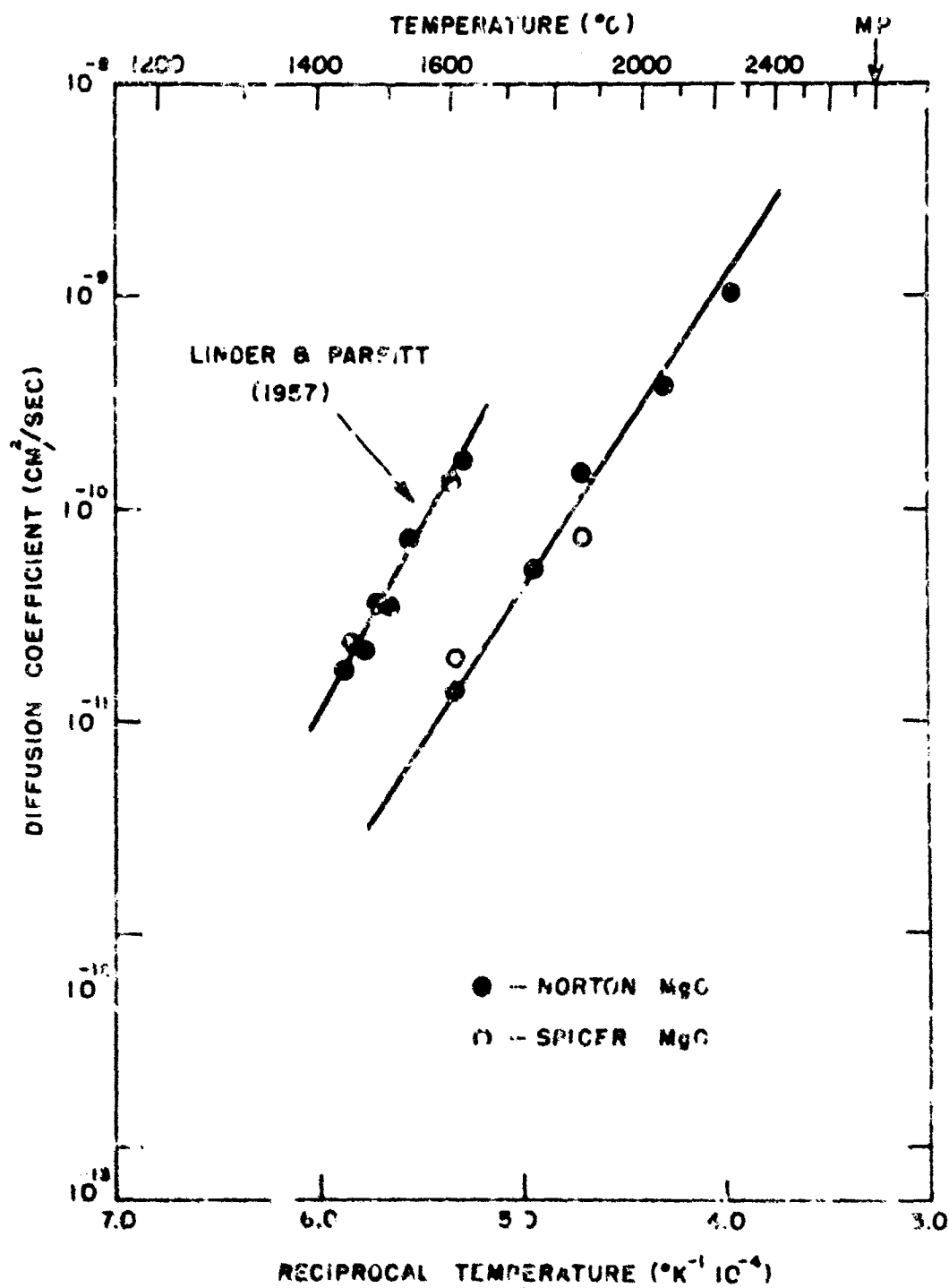


Figure 2.  
Plot of ionic self-diffusion coefficients in single crystal MgO as a function of reciprocal temperature.

diffusion.

#### IV. REFERENCES

1. S.P. Mitoff, J. Chem. Phys., 31, 1261 (1959).
2. M.O. Davies, J. Chem. Phys., 38, 2047 (1963).
3. H. Schmalzried, Z. Physik. Chem. 38, 87 (1960).
4. S.P. Mitoff, J. Chem. Phys., 36, 1383 (1962).
5. Y. Oishi and W.D. Kingery, J. Chem. Phys., 33, 905 (1960).
6. R. Lindner and G.D. Parfitt, J. Chem. Phys., 26, 182 (1957).
7. B.C. Harding and A.J. Mortlock, J. Chem. Phys., 45, 2699 (1966).
8. H. Togai, S. Iwai, T. Iseki and M. Saho, Radex Rundschau, 4, 577 (1965).
9. B.J. Wuensch and T. Vasilos, J. Chem. Phys., 36, 2917 (1962).
10. B.J. Wuensch and T. Vasilos, J. Chem. Phys., 42, 4113 (1965).
11. J. Rungis and A.J. Mortlock, Phil. Mag., 14, 821 (1966).
12. B.J. Wuensch and T. Vasilos, N.B.S. Spec. Pub. 296, 95 (1968).
13. B.C. Harding, Phil. Mag., 16, 1039 (1967).
14. J. Yamashita and T. Kurosawa, J. Phys. Soc. Japan 9, 944 (1951).
15. Interim Report AVSD-0402-70-CR, Contract DANC 15-68-C-0296 (15 June 1970).
16. H. Schafer and A. Tebben, Z. Anorg. Allgem. Chem. 304, 317 (1960).
17. G.W. Hooper and P. Hautefeuille, Compt. Rend. Acad. Sci. 84, 946 (1877).
18. I. Zaplatynsky, J. Am. Ceram. Soc., 45, 28 (1962).
19. J.S. Choi, Ph.D. Thesis, Indiana University (1963).
20. S.L. Blank and J.A. Pask, J. Am. Ceram. Soc., 52, 699 (1969).
21. J.W. Cleland, N.B.S. Spec. Pub. 296, 195 (1968).

UNCLASSIFIED

Security Classification

DOCUMENT CONTROL DATA - R&D		
(Security classification of title, body of abstract and indexing annotation must be entered when the overall report is classified)		
1. ORIGINATING ACTIVITY (Corporate author) Avco Corporation, Systems Division, Materials Sciences Dept. Lowell Industrial Park, Lowell, Massachusetts 01851		2a. REPORT SECURITY CLASSIFICATION Unclassified
3. REPORT TITLE  Transport Processes in Ceramic Oxides		2b. GROUP
4. DESCRIPTIVE NOTES (Type of report and inclusive dates) Semi-Annual Technical Report, 16 June 1970 - 15 December 1970		
5. AUTHOR(S) (Last name, first name, initial) Vasilos, Thomas      Gruber, Philip E. Wuensch, Bernhardt      Rhodes, William H.		
6. REPORT DATE 15 December 1970	7a. TOTAL NO. OF PAGES 31	7b. NO. OF REFS 21
8a. CONTRACT OR GRANT NO. DAHCL5-68-C-0296	8b. ORIGINATOR'S REPORT NUMBER(S) AVSD-0092-71-CR	
a. PROJECT NO. 1130		
c. 8D10		
10. AVAILABILITY/LIMITATION NOTICES Reproduction in whole or in part is permitted for any purpose of the U.S. Government. Distribution of this document is unlimited.		
11. SUPPLEMENTARY NOTES	12. SPONSORING MILITARY ACTIVITY Materials Research Division Advanced Research Projects Agency Arlington, Virginia	
13. ABSTRACT Progress is described in a program intended to clarify the nature of mass transport in MgO through (1) growth of crystals of improved perfection and purity, (2) measurement of cation self-diffusion rates over a wide range of temperatures, and (3) extension of diffusion measurements as close as possible to the melting point of the material.  Crystals of MgO 2 cm in diameter and 2 mm in thickness are routinely and reproducibly grown epitaxially on MgO substrates by means of chemical vapor transport with HCl at 1000°C. Growth rates of 90 micron/hr. have been achieved. Crystals grown from high purity source material contain 400 ppm total impurity. Primary offenders are Fe, Si, and S, but it appears possible to further reduce levels of these elements. Measurements of Ni <sup>2+</sup> diffusion in MgO have been extended to 2460°C (0.88 T <sub>m</sub> ) in an attempt to reveal intrinsic transport. The measurements extend by 70% the temperature range over which transport data for MgO are now available, but fail to reveal a change in transport mechanism. Ni <sup>2+</sup> diffusion at high temperatures may be adequately described by a D <sub>0</sub> of 1.80 10 <sup>-5</sup> cm <sup>2</sup> /sec and an activation energy of 2.10 eV, a result obtained through earlier measurements at much lower temperatures. Mg <sup>2+</sup> self-diffusion in MgO in the temperature range 1600°-2250°C may be represented by a D <sub>0</sub> of 9.52 10 <sup>-4</sup> cm <sup>2</sup> /sec and an activation energy of 2.92 eV. The results are interpreted as extrinsic diffusion and are not in accord with limited data in the literature for diffusion of the radioisotope Mg <sup>28</sup> . Neither of the present diffusion studies has revealed a significant difference between transport in moderate purity crystals and ( )		

DD FORM 1473

crystals of the best quality which are commercially available.

UNCLASSIFIED

Security Classification

new studied.

UNCLASSIFIED

## Security Classification

14. KEY WORDS	LINK A		LINK B		LINK C	
	ROLE	WT	ROLE	WT	ROLE	WT
Diffusion, $Mg^{2+}$ in $MgO$ ; $Ni^{2+}$ in $MgO$ Cation self-diffusion Impurity ion diffusion, $Ni^{2+}$ in $MgO$ Crystal growth Chemical vapor deposition						

**INSTRUCTIONS**

1. **ORIGINATING ACTIVITY:** Enter the name and address of the contractor, subcontractor, grantee, Department of Defense activity or other organization (corporate author) issuing the report.

2a. **REPORT SECURITY CLASSIFICATION:** Enter the overall security classification of the report. Indicate whether "Restricted Data" is included. Marking is to be in accordance with appropriate security regulations.

2b. **GROUP:** Automatic downgrading is specified in DoD Directive 5200.10 and Armed Forces Industrial Manual. Enter the group number. Also, when applicable, show that optional markings have been used for Group 3 and Group 4 as authorized.

3. **REPORT TITLE:** Enter the complete report title in all capital letters. Titles in all cases should be unclassified. If a meaningful title cannot be selected without classification, show title classification in all capitals in parentheses immediately following the title.

4. **DESCRIPTIVE NOTES:** If appropriate, enter the type of report, e.g., interim, progress, summary, annual, or final. Give the inclusive dates when a specific reporting period is covered.

5. **AUTHOR(S):** Enter the name(s) of author(s) as shown on or in the report. Enter last name, first name, middle initial. If military, show rank and branch of service. The name of the principal author is an absolute minimum requirement.

6. **REPORT DATE:** Enter the date of the report as day, month, year; or month, year. If more than one date appears on the report, use date of publication.

7a. **TOTAL NUMBER OF PAGES:** The total page count should follow normal pagination procedures, i.e., enter the number of pages containing information.

7b. **NUMBER OF REFERENCES:** Enter the total number of references cited in the report.

8a. **CONTRACT OR GRANT NUMBER:** If appropriate, enter the applicable number of the contract or grant under which the report was written.

8b, 8c, & 8d. **PROJECT NUMBER:** Enter the appropriate military department identification, such as project number, subject number, system number, task number, etc.

9a. **ORIGINATOR'S REPORT NUMBER(S):** Enter the official report number by which the document will be identified and controlled by the originating activity. This number must be unique to this report.

9b. **OTHER REPORT NUMBER(S):** If the report has been assigned any other report number (either by the originator or by the sponsor), also enter this number(s).

10. **AVAILABILITY/LIMITATION NOTICES:** Enter any limitations on further dissemination of the report, other than those imposed by security classification, using standard statements such as:

- (1) "Qualified requesters may obtain copies of this report from DDC."
- (2) "Foreign announcement and dissemination of this report by DDC is not authorized."
- (3) "U. S. Government agencies may obtain copies of this report directly from DDC. Other qualified DDC users shall request through \_\_\_\_\_."
- (4) "U. S. military agencies may obtain copies of this report directly from DDC. Other qualified users shall request through \_\_\_\_\_."
- (5) "All distribution of this report is controlled. Qualified DDC users shall request through \_\_\_\_\_."

If the report has been furnished to the Office of Technical Services, Department of Commerce, for sale to the public, indicate this fact and enter the price, if known.

11. **SUPPLEMENTARY NOTES:** Use for additional explanatory notes.

12. **SPONSORING MILITARY ACTIVITY:** Enter the name of the departmental project office or laboratory sponsoring (paying for) the research and development. Include address.

13. **ABSTRACT:** Enter an abstract giving a brief and factual summary of the document indicative of the report, even though it may also appear elsewhere in the body of the technical report. If additional space is required, a continuation sheet shall be attached.

It is highly desirable that the abstract of classified reports be unclassified. Each paragraph of the abstract shall end with an indication of the military security classification of the information in the paragraph, represented as (TS), (S), (C), or (U).

There is no limitation on the length of the abstract. However, the suggested length is from 150 to 225 words.

14. **KEY WORDS:** Key words are technically meaningful terms or short phrases that characterize a report and may be used as index entries for cataloging the report. Key words must be selected so that no security classification is required. Identifiers, such as equipment model designation, trade name, military project code name, geographic location, may be used as key words but will be followed by an indication of technical content. The assignment of links, rules, and weights is optional.

UNCLASSIFIED

Security Classification